Quantum Electronics **47** (6) 561–566 (2017)

BIOPHOTONICS

https://doi.org/10.1070/QEL16378

Study of the epidermis ablation effect on the efficiency of optical clearing of skin *in vivo**

E.A. Genina, N.S. Ksenofontova, A.N. Bashkatov, G.S. Terentyuk, V.V. Tuchin

Abstract. **We present the results of a comparative analysis of optical immersion clearing of skin in laboratory animals *in vivo* with and without preliminary ablation of epidermis. Laser ablation is implemented using a setup based on a pulsed erbium laser (λ = 2940 nm). The size of the damaged region amounted to 6 × 6 mm, the depth being smaller than 50 μm. As an optical clearing agent (OCA), use is made of polyethylene glycol (PEG-300). Based on optical coherence tomography, we use the single scattering model to estimate the scattering coefficient in the process of optical clearing in 2 regions at depths of 50–170 μm and 150–400 μm. The results show that skin surface ablation leads to the local oedema of the affected region that increases the scattering coefficient. However, the intense evaporation of water from the ablation zone facilitates the optical clearing at the expense of tissue dehydration, particularly in the upper layers. The assessment of the optical clearing efficiency shows that the efficiency exceeding 30% can be achieved at a depth from 50 to 170 μm in 120 min after ablation, as well as after the same ablation with subsequent application of PEG-300, which increases the efficiency of the immersion method by almost 1.8 times. At a depth from 150 to 400 μm, dehydration of upper layers cannot completely compensate for an increase in light scattering by dermis after epidermis ablation. The additional effect of OCA enhances the optical clearing of skin at the expense of improving the refractive index matching between dermis components, but the maximal efficiency of optical clearing in 120 min does not exceed 6%.**

Keywords: *laser ablation, optical clearing of skin, optical coherence tomography.*

*Presented at the Fundamentals of Laser-Assisted Micro- and Nanotechnologies (FLAMN-16) International Symposium (Pushkin, Leningrad oblast, 27 June to 1 July 2016).

E.A. Genina, A.N. Bashkatov Saratov State University, ul. Astrakhanskaya 83, 410012 Saratov, Russia; National Research Tomsk State University, prosp. Lenina 36, 634050 Tomsk, Russia; eagenina@yandex.ru;
N.S. Ksenofontova Saratov State University, ul. Astrakhanskaya 83, 410012 Saratov, Russia;
G.S. Terentyuk The First Veterinary Clinic, ul. Astrakhanskaya 98, 410012 Saratov, Russia;
V.V. Tuchin Saratov State University, ul. Astrakhanskaya 83, 410012 Saratov, Russia; National Research Tomsk State University, prosp. Lenina 36, 634050 Tomsk, Russia; Institute of Problems of Precise Mechanics and Control, Russian Academy of Sciences, ul. Rabochaya 24, 410028 Saratov, Russia; e-mail: tuchinvv@mail.ru

Received 24 March 2017
Kvantovaya Elektronika **47** (6) 561–566 (2017)
Translated by V.L. Derbov

1. Introduction

Transepidermal and transdermal delivery of medicinal preparations and optical immersion agents attracts great attention of the researchers. A number of papers in this field is devoted to the development of methods aimed to overcome the epidermal barrier that hampers free diffusion of preparations from the surface to deeper skin layers [1–7]. Due to the presence of the epidermis stratum corneum having a thickness of 10–20 μm and consisting of densely packed keratinised corneocytes surrounded by a lipid matrix, only small lipophilic molecules (with a molecular mass below 500 Da) can freely diffuse through the intact epidermis [7]. The diffusion of water molecules through the epidermis stratum corneum is hampered by the tortuosity of transport paths in the intercellular space and strongly depends on the degree of its hydration [8].

Among optical clearing agents (OCAs) the most efficient ones for skin are hydrophilic preparations rather than lipophilic ones [9], since the dominant contribution to the light scattering by skin is introduced by dermis, and the dominant liquid in dermis is water. Therefore, the implementation of the transport of hydrophilic OCAs through the epidermal barrier to dermis is an urgent problem.

The chemical method, aimed at dissolving the lipid matrix of the stratum corneum and producing pores in it, belongs to the most widespread methods of OCA diffusion enhancement [10, 11]. Sonophoresis [12] and microperforation of epidermis by means of microneeldle arrays [13] are often used, as well as combinations of physical and chemical impacts [14–16]. A number of papers are also devoted to the effect of pulsed laser radiation and photothermal action on the epidermis permeability [4, 5, 17–22].

Laser ablation (LA) is an efficient and safe method that produces thermal microdamages of different depth and diameter depending on the laser impact parameters [4, 5, 19, 22–27]. These papers are devoted to the study of delivering medicinal preparations, macromolecules, micro- and nanoparticles either through ablation channels, penetrating through the epidermis and part of dermis (to a depth down to 400 μm), or through comparatively large areas of the ablated epidermis surface. The obtained results confirm the efficiency of using LA for enhancing the epidermis permeability for the studied agents. However, the use of LA to enhance the OCA diffusion into the dermis is studied insufficiently. Previously in our work [28] we performed a preliminary study of the time dependence of the skin optical probing depth using optical coherence tomography (OCT) after the fractional microablation of the skin surface with subsequent application of different OCAs. The results demonstrated the reduction of the skin probing depth immediately after ablation, with its subsequent

growth during an hour to the value, obtained in the intact skin before ablation (i.e., the absence of the optical clearing effect). The obtained results demonstrate the necessity of a more detailed study of optical clearing mechanisms in skin with ablated epidermis.

Thus, the aim of the present paper is a comparative study of the optical immersion clearing of skin in laboratory animals *in vivo* using hydrophilic OCAs with and without preliminary epidermis ablation.

2. Materials and methods

LA was performed using a setup based on a StarLux/Lux2940 Er:YAG laser (Palomar Medical Technologies Inc., Burlington, USA), combined with a Booster-2 module (Laser Centre, ITMO University, Russia), generating pulses with the following parameters: radiation wavelength of 2940 nm, pulse energy of 1 J and single-spike pulse structure with a spike duration of 200 μs.

The surface skin layer area with a size of 6 × 6 mm and a damage depth smaller than 50 μm was ablated by a wide beam.

To study the skin optical clearing we used polyethylene glycol with a molecular weight of 300 (PEG-300) (Sigma-Aldrich, USA). Due to its efficiency, availability and biocompatibility, PEG-300 is widely used as an OCA [16, 29–32]. The refractive index of PEG-300 at a wavelength of 930 nm is 1.456 [32].

The measurements were performed *in vivo* in 15 laboratory albino rats, which were divided into 3 groups, 5 animals in each. In group I only LA was executed, in group II PEG-300 was applied on intact skin, and in group III LA was followed by a single application of PEG-300 on the skin surface. The agent layer thickness amounted to approximately 50 ± 20 μm. The OCT images made it possible to estimate the agent layer thickness, the axial resolution of the tomograph being ~9 μm in the medium with a refractive index of 1.456. The age of the animals was 1 year; the mass was 200–300 g. Before the experiment, the animals were subjected to anaesthesia by intramuscular injection of 0.18–0.2 mL of Zoletil 50 (Vibrac, France). The hair was removed from the skin surface using 'Veet' depilatory cream (Reckitt Benckiser, France).

The skin condition in the process of optical clearing was monitored using a Thorlabs OCP930R spectral optical coherence tomograph (Thorlabs, USA) having the following parameters: centre radiation wavelength of 930 ± 5 nm; axial and lateral resolution of 6.2 and 9.6 μm, respectively; and scanning region length of 2 mm. The OCT signals of the processed region were recorded before ablation and immediately after it and/or the PEG-300 application, every 2–5 min during 100–120 min.

Uisng the single scattering model [33, 34], the attenuation coefficient μ_t was estimated by the slope of the OCT scans [16]. According to the single scattering model, the power of the detected OCT signal $R(z)$ is proportional to $\exp(-\mu_t z)$ [35]. Since in the studied spectral range the absorption coefficient μ_a of skin is much smaller than the scattering coefficient μ_s [36], the attenuation coefficient $\mu_t = \mu_s + \mu_a$ can be assumed approximately equal to the scattering coefficient. Therefore, the OCT signal $R(z)$ can be approximated by the expression

$$R(z) = A\exp(-\mu_s z) + B, \quad (1)$$

where A is the proportionality factor, equal to $P_0\alpha(z)$; P_0 is the optical power of the beam, incident on the tissue surface; $\alpha(z)$ is determined by the local backscattering capability of the tissue and depends on the local variation of the refractive index; and B is the background signal.

Figure 1 presents the analysed regions of the OCT image, the averaged A-scan of the OCT signal from the dermal layer of the rat skin *in vivo* and the approximating curve obtained using the single scattering model. The OCT signals were averaged over 101 scans sweeping the skin region ~300 μm long. The values of the scattering coefficient were determined in two regions of the averaged A-scan. Region 1 corresponded to a depth from 50–70 μm to 150–170 μm (depending on the specific features of a particular sample). Region 2 corresponded to a depth from 150–170 μm to 350–400 μm. The values of μ_s were calculated for each animal separately and averaged over the group for each measurement time. Then the appropriate standard deviation was estimated.

The optical clearing efficiency (OCE) was estimated for each studied region separately using the following expression

$$\mathrm{OCE} = \frac{\mu_s(t=0) - \mu_s(t)}{\mu_s(t=0)} \times 100\%, \quad (2)$$

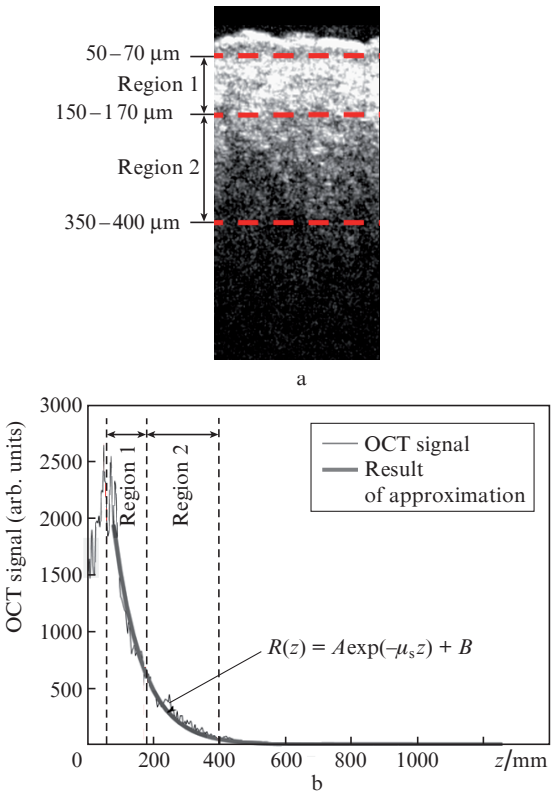

Figure 1. Measurements of the scattering coefficient μ_s at the regions of dermis with a depth from 50–70 μm to 150–170 μm (region 1) and from 150–170 μm to 350–400 μm (region 2) based on the analysis of the averaged OCT signal depth distribution using the single scattering model; (a) B-scan of the skin *in vivo*, measured immediately after ablation, with a length of ~300 μm, (101 A-scans), over which the averaging of the OCT signal was performed, (b) the depth distribution of the averaged OCT signal (thin curve) and the result of approximation according to the single scattering model (thick curve). The dashed straight lines indicate the boundaries of the regions, where the values of μ_s were estimated.

where $\mu_s(t)$ is the current value of the scattering coefficient averaged over the group; and $\mu_s(t = 0)$ is the initial value of the scattering coefficient averaged over the group (for intact skin). The OCE values were calculated for each animal separately, averaged over the group at each time of OCT recording, and then the appropriate standard deviation was calculated.

3. Results and discussion

Figure 2 presents OCT images of the studied skin region for group I of the experimental animals with ablated epidermis and the kinetics of the averaged scattering coefficient for two regions located at different depths. The zero of the time scale corresponds to the OCT signal recording immediately after ablation. The initial values of μ_s, located in the negative part of the time scale, correspond to the intact skin before the impact. In Fig. 2a, it is clearly seen that the probed region (i.e., the light area in the OCT image that corresponds to the illuminated region inside the tissue) decreases immediately after ablation and then begins to grow. Correspondingly, the scattering coefficient after ablation considerably exceeds the initial values (for intact skin) in both regions (Fig. 2b). The maximal change in the coefficient μ_s (an increase by 60%) is achieved in region 1, i.e., at a depth from 50 to 170 μm. This is related to an increase in light scattering by the tissue due to oedema, the influx of the interstitial fluid (water) and lymph to the damaged zone, which is a response of the organism to the skin damage, the oedema near the damaged zone being greater than in deeper layers. In region 2, the value of μ_s increases on average by 30%. Then, a rather sharp fall (during 6–8 min) almost to the initial values is observed for the scattering coefficient in both regions, which is due to the intense evaporation of water from the skin surface in the zone devoid of the protective action of the epidermis stratum corneum.

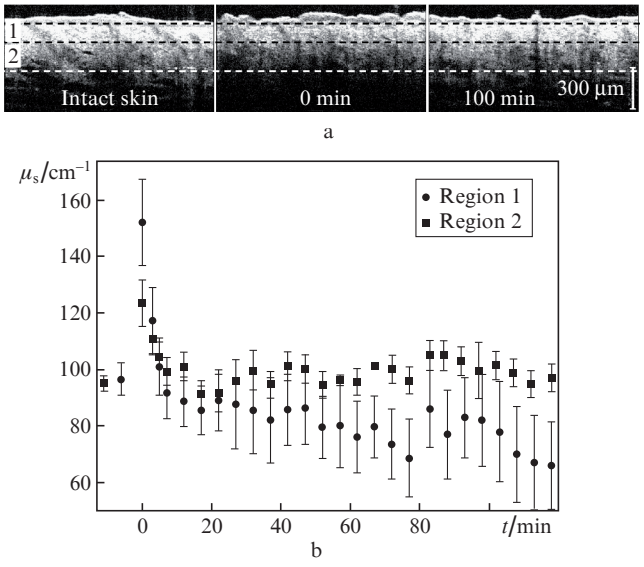

Figure 2. (a) Typical OCT images of the studied skin region in group I of the experimental animals, subjected to ablation of epidermis at different time periods and (b) time dependences of the averaged scattering coefficient in two regions, corresponding to different depths inside the skin: region 1 – the depth from 50–70 μm to 150–170 μm, region 2 – from 150–170 μm to 350–400 μm. The dashed lines in the OCT images show the boundaries of the regions.

Then, the evaporation of water continues at a lower rate, and the dehydrated layer appears at the surface in the ablation zone. In this layer both the refractive index of the liquid is higher (i.e., the dehydration immersion occurs) and the tissue fibrils are packed denser than in the intact tissue, which leads to a gradual decrease in light scattering in region 1 (on average by 56%). In region 2, the evaporation from the skin surface is likely to have no essential effect on the values of μ_s. The scattering coefficient fluctuates near the value, slightly exceeding the initial one, since during the observation time a sufficient oedema remains in the skin.

In the literature, there is a disagreement about the assessment of the scattering coefficient in the tissues with oedema in comparison with healthy tissues. On the one hand, Phillips et al. [37] report a slight increase in the light scattering coefficient in dermis with the oedema caused by psoriasis. On the other hand, the authors of Refs [38, 39] show that the scattering of light in the skin dermis with psoriasis and contact dermatitis, accompanied by the dermis oedema, is smaller than in healthy skin. According to these papers, this is due to a decreased density of collagen fibres in the oedema region. In our opinion, this difference may be due to the specific features of the oedema. In Ref. [38], the oedema in dermis was accompanied by an increase in the epidermis thickness approaching 20%, which is a sign of strongly expressed oedema. In Ref. [39], due to the oedema the tissue volume increased by up to 15 times. In this case, the key role was played by the packing density of collagen fibres in dermis, which considerably decreased with increasing significantly tissue volume. Besides that, the increased content of water in the interstitial matrix can increase the hydration of the dermis fibres, which, in turn, decreases their refractive index [40, 41] and facilitates better matching of refractive indices of the fibres and the interstitial matrix. As follows from Ref. [38], the observation of the oedema development continued during 7 days. During such a long time, the above modifications can occur in the hydration of the fibres. In contrast to the results of papers [38, 39], in our work the oedema was caused by a sight damage of epidermis, developed during a few minutes, and was observed during less than two hours. In this case, the oedema was not strongly expressed. No increase in the epidermis thickness was observed in the OCT images and, therefore, the influx of water to the ablation zone mainly facilitated the decrease in the refractive index of the interstitial fluid, i.e., the additional mismatch of refractive indices of dermis components, which resulted in the increase in light scattering in the tissue.

Figure 3 presents OCT images of the studied skin region and time dependences of the averaged scattering coefficient at two different depths in the skin of experimental animals belonging to group II. In this group, no ablation was carried out and only the OCA was applied to skin. The zero of the time scale corresponds to the moment of PEG-300 application, the negative time values, as in the previous group, correspond to the period preceding the impact. From Fig. 3a it follows that the optical depth of the skin probing region increased immediately after OCA application, and after that its temporal variations were insignificant. However, in Fig. 3b it is clearly seen that the time variations of μ_s at different depths are different. In the near-surface layer, a sharp decrease in μ_s is observed (on average by 26%) during the first 25 min, which, in our opinion, is mainly caused by the immersion of the epidermis stratum corneum surface. Then, the immersion agent impregnates the epidermis and the near-surface dermis layers, but its concentration decreases because of mixing with

the interstitial fluid; besides that, the agent is removed from the observation zone by diffusion to the surrounding tissue. Hence, the value of μ_s gradually increases with time. At a depth of 150–400 μm (region 2) the decrease in μ_s is slower and begins in 20–30 min, i.e., after the impregnation of the epidermis, too. Nearly in 1.5 h the values of μ_s in both regions become equalised, which is a sign of a uniform PEG-300 distribution in the interstitial fluid in the detection zone.

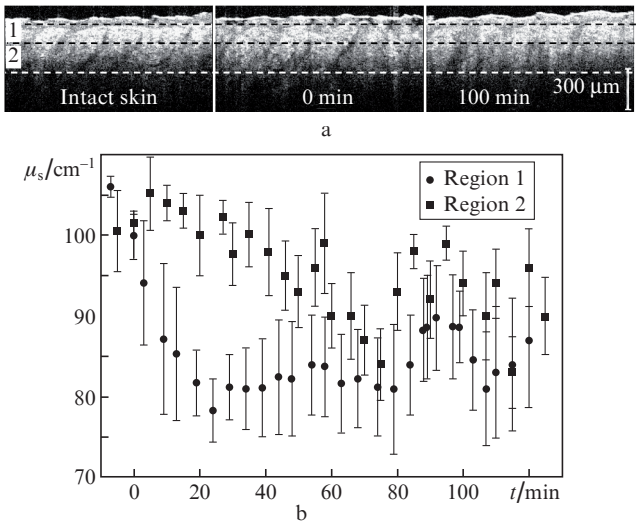

Figure 3. (a) Typical OCT images of the studied skin region in group II of the experimental animals, after the application of the immersion agent on the intact skin surface at different time periods and (b) time dependences of the averaged scattering coefficient in two regions, corresponding to different depths inside the skin: region 1 – the depth from 50–70 μm to 150–170 μm, region 2 – from 150–170 μm to 350–400 μm. The dashed lines in the OCT images show the boundaries of the regions.

Figure 4 presents the OCT images of the studied skin region and the kinetics of the scattering coefficient variation after the epidermis ablation followed by application of the immersion agent (group III of laboratory animals). The zero of the time scale corresponds to the moment of PEG-300 application. In the region of negative time values, the scattering coefficient corresponds to the intact skin. In this case, we expect two competing processes to occur: on the one hand, the skin oedema near the damaged zone causes an increase in μ_s, and on the other hand, the immersion decreases scattering and, therefore, μ_s should decrease. As follows from Fig. 4a, the application of the immersion agent practically does not reduce the skin probing region after ablation, as was observed in group I (see Fig. 2a). In Fig. 4b it is also clearly seen that in region 1, corresponding to the near-surface layer of skin, there is no sharp increase in the scattering coefficient, as it happens in the case of skin ablation without applying the immersion agent (see Fig. 2b). On the contrary, μ_s gradually decreases (on average by 25%), achieves a minimum during an hour and then fluctuates near this value.

Thus, under the OCA effect immediately after the application, the immersion of the dermis upper layer occurs, reducing the influence of the water influx to the ablated region on the scattering coefficient. The presence of the tissue oedema is indirectly confirmed by the kinetics of μ_s at a depth from 150 to 400 μm. At the expense of an increasing water content in

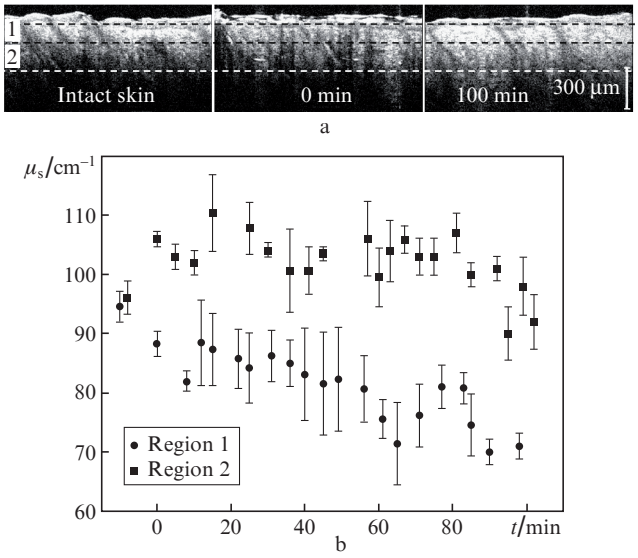

Figure 4. (a) Typical OCT images of the studied skin region in group III of the experimental animals, after the epidermis ablation and application of the immersion agent on the ablation zone at different time periods and (b) time dependences of the averaged scattering coefficient in two regions, corresponding to different depths inside the skin: region 1 – the depth from 50–70 μm to 150–170 μm, region 2 – from 150–170 μm to 350–400 μm. The dashed lines in the OCT images show the boundaries of the regions.

surrounding tissues, the coefficient μ_s increases during the first minutes of observation, and in 90 min exceeds the initial value on average by 8%. Generally, the kinetics of μ_s under the conditions of ablation and immersion coincides with that of the tissue scattering coefficient in the case of ablation without applying the immersion agent (see Fig. 2b). However, in contrast to the pure dehydration mechanism of optical clearing that takes the place in the case of epidermis ablation, after the OCA application the additional matching occurs in the dermis between the refractive indices of the scatterers (collagen fibres) and the interstitial fluid, into which PEG-300 penetrates. The total decrease in μ_s after ablation in groups I and III amounts to 15% and 20%, respectively. In the OCT images, it is also clearly seen that the optical depth of the illuminated region inside the tissue in Fig 4a is larger than that in Fig. 2a.

The above effects are clearly demonstrated in Fig. 5, where the values of the skin optical clearing efficiency in different experimental groups, calculated using Eqn (2) for a few time intervals are presented. In Fig. 5a, one can see that in the near-surface layer (at a depth down to 150–170 μm) the maximal efficiency in 30 min after the beginning of the impact is demonstrated by the immersion method of optical clearing. The methods related to ablation are less efficient because of the increased scattering in skin due to oedema. Then, in the process of optical clearing, the efficiency of the pure immersion method decreases (due to the reduction of the OCA concentration in the process of filling a large volume of a tissue), and the efficiency of methods incorporating ablation grows (due to dehydration). Thus, in 60 min after the beginning of observation, all three methods show approximately equal efficiency, and in 120 min the efficiency of ablation methods exceeds that of the immersion method almost by 1.8 times. It is interesting to note that in the near-surface layer the combined effect of ablation and immersion yields practically no

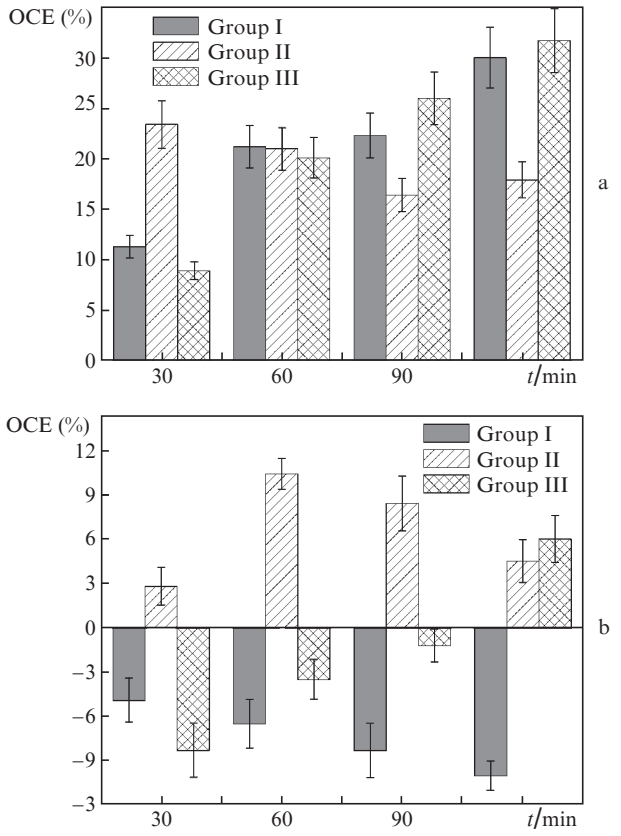

Figure 5. Time dependences of the skin optical clearing efficiency in three studied groups of experimental animals at a depth (a) from 50–70 μm to 150–170 μm and (b) from 150–170 μm to 350–400 μm.

additional increase in efficiency of optical clearing, as compared to dehydration.

In deeper layers (150–400 μm), the maximal efficiency of optical clearing is attained in 60 min after the OCA application (Fig. 5b) Then, it also begins to decrease, while the efficiency of the combined optical clearing method gradually increases. In 120 min, the efficiency is maximal in the group with ablation + immersion, but its absolute value is almost by 2 times smaller than the efficiency of optical clearing caused solely by the OCA at the 60th minute of the experiment. The efficiency caused by evaporation in the ablation zone is reduced during every subsequent time interval because of the increased scattering, which can be an evidence in favour of the increased oedema in deep layers of dermis.

4. Conclusions

The studies have shown that the use of laser ablation aimed at the enhancement of diffusion of hydrophilic agents into the skin is accompanied by increased light scattering in dermis due to the influx of the interstitial fluid and lymph to the damage site. However, in the near-surface layers of skin (at a depth down to 150–170 μm) the effect of the increased light scattering in the tissue is compensated for by intense evaporation of water via the damage zone. In this case, the additional application of the immersion agent has no essential effect on the degree of optical clearing. Thus, the effect of the dehydration mechanism increases the efficiency of optical clearing, as compared to the purely immersion one, by almost 1.8 times during 120 min. In deeper skin layers (from 150 to 400 μm) in the case of ablation a light scattering increase is also observed, but it cannot be compensated for by the dehydration of the upper layers only. The additional effect of the OCA increases optical clearing of skin at the expense of better matching of refractive indices of dermis components, but the maximal efficiency of optical clearing does not exceed 6%. In this case, it may possible to increase the efficiency of optical clearing by taking the OCAs with greater refractive indices, e.g., glycerol.

Acknowledgements. The authors express their gratitude to L.E. Dolotov for help in the experiments and A.B. Bucharskaya for providing with laboratory animals. E.A. Genina and V.V. Tuchin acknowledge the support of the Grants Council of the Government of Russia (State Support of Research Carried out under the Supervision of Leading Scientists Programme, Grant No. 14.Z50.31.0004). The work of A.N. Bashkatov was partially supported by the Russian Science Foundation (Grant No. 14-15-00186). N.S. Ksenofontova acknowledges the support of the RF President's Grants Council (State Support to Leading Scientific Schools Programme, Grant No. NSh-7898.2016.2).

References

1. Cross S.E., Roberts M.S. *Cur. Drug Deliv*., **1** (1), 81 (2004).
2. Benson H.A.E. *Cur. Drug Deliv*., **2** (1), 23 (2005).
3. Tanner T., Marks R. *Skin Res. Technol*., **14**, 249 (2008).
4. Bachhav Y.G., Summer S., Heinrich A., Bragagna T., Bohler C., Kalia Y.N. *J. Control. Release*, **146** (1), 31 (2010).
5. Lin C.-H., Aljuffali I.A., Fang J.-Y. *Expert Opin. Drug Deliv*., **11** (4), 599 (2014).
6. Azagury A., Khoury L., Enden G., Kost J. *Adv. Drug Deliv. Rev*., **72**, 127 (2014).
7. Brown M.B., Martin G.P., Jones S.A., Akomeah F.K. *Drug Deliv*., **13** (3), 175 (2006).
8. Blank I.H., Moloney J., Emslie A.G., Simon I., Apt C. *J. Invest. Dermatol*., **82** (2), 188 (1984).
9. Choi B., Tsu L., Chen E., Ishak T.S., Iskandar S.M., Chess S., Nelson J.S. *Lasers Surg. Med*., **36** (2), 72 (2005).
10. Andanson J.M., Chan K.L.A., Kazarian S.G. *Appl. Spectros*., **63** (5), 512 (2009).
11. Wen X., Jacques S.L., Tuchin V.V., Zhu D. *J. Biomed. Opt*., **17** (6), 066022 (2012).
12. Xu X., Zhu Q., Sun C. *J. Biomed. Opt*., **14** (3), 034042 (2009).
13. Yoon J., Son T., Choi E., Choi B., Nelson J.S., Jung B. *J. Biomed. Opt*., **13** (2), 021103 (2008).
14. Yoon J., Park D., Son T., Seo J., Nelson J.S., Jung B. *Lasers Surg. Med*., **42**, 412 (2010).
15. Zhong H., Guo Z., Wei H., Guo L., Wang C., He Y., Xiong H., Liu S. *Photochem. Photobiol*., **86**, 732 (2010).
16. Genina E.A., Bashkatov A.N., Kolesnikova E.A., Basko M.V., Terentyuk G.S., Tuchin V.V. *J. Biomed. Opt*., **19** (2), 021109 (2014).
17. Lee S., McAuliffe D.J., Flotte T.J., Kollias N., Doukas A.G. *Lasers Surg. Med*., **28**, 344 (2001).
18. Gomez C., Costela A., Garcia-Moreno I., Llanes F., Teijon J.M., Blanco D. *Lasers Surg. Med*., **40**, 6 (2008).
19. Haak C.S., Farinelli W.A., Tam J., Doukas A.G., Anderson R.R., Haedersdal M. *Lasers Surg. Med*., **44**, 787 (2012).
20. Liu C., Zhi Z., Tuchin V.V., Luo Q., Zhu D. *Lasers Surg. Med*., **42**, 132 (2010).
21. Genina E.A., Bashkatov A.N., Tuchin V.V., Simonenko G.V., Sherstneva V.N., Yaroslavsky I.V., Altshuler G.B. *J. Innov. Opt. Health Sci*., **2** (3), 279 (2009).
22. Nelson J.S., McCullough J.L., Glenn T.C., Wright W.H., Liaw L.-H.L., Jacques S.L. *J. Invest. Dermatol*., **97** (5), 874 (1991).
23. Garvie-Cook H., Stone J.M., Yu F., Guy R.H., Gordeev S.N. *J. Biophot*., **9** (1–2), 144 (2016).
24. Aljuffali I.A., Lin C.-H., Fang J.-Y. *J. Drug Del. Sci. Tech*., **24**, 277 (2014).

25. Jang H.-J., Hur E., Kim Y., Lee S.-H., Kang N.G., Yoh J.J. *J. Biomed. Opt*., **19**, 118002 (2014).
26. Chang H.-C., Lin Y.-H., Huang K.-C. *J. Innov. Opt. Health Sci*., **8**, 1550029 (2015).
27. Genina E.A., Dolotov L.E., Bashkatov A.N., Tuchin V.V. *Quantum Electron*., **46** (6), 502 (2016) [*Kvantovaya Elektron*., **46** (6), 502 (2016)].
28. Kolesnikova E.A., Kolesnikov A.S., Genina E.A., Dolotov L.E., Tuchina D.K., Bashkatov A.N., Tuchin V.V. *Proc. SPIE*, **8699**, 8699 0B (2013).
29. Mao Z., Zhu D., Hu Y., Wen X., Han Z. *J. Biomed. Opt*., **13** (2), 021104 (2008).
30. Ding Y., Wang J., Fan Z., Wei D., Shi R., Luo Q., Zhu D., Wei X. *Biomed. Opt. Express*, **4** (11), 2518 (2013).
31. Zhong H., Guo Z., Wei H., Guo L., Wang C., He Y., Xiong H., Liu S. *Photochem. Photobiol*., **86**, 732 (2010).
32. Tuchina D.K., Genin V.D., Bashkatov A.N., Genina E.A., Tuchin V.V. *Opt. Spectrosc*., **120** (1), 28 (2016) [*Opt. Spektrosk*., **120** (1), 36 (2016)].
33. Faber D.J., van der Meer F.J., Aalders M.C.G., van Leeuwen T.G. *Opt. Express*, **12** (19), 4353 (2004).
34. Lee P., Gao W., Zhang X. *Appl. Opt*., **49** (18), 3538 (2010).
35. Wang R.K., Tuchin V.V., in *Handbook of Coherent-Domain Optical Methods. Biomedical Diagnostics, Environmental Monitoring, and Material Science*. Ed. by V.V. Tuchin (New York, Heidelberg, Dordrecht, London: Springer, 2013) Vol. 2, p. 665.
36. Bashkatov A.N., Genina E.A., Tuchin V.V. *J. Innov. Opt. Health Sci*., **4** (1), 9 (2011).
37. Phillips K.G., Wang Y., Levitz D., Choudhury N., Swanzey E., Lagowski J., Kulesz-Martin M., Jacques S.L. *J. Biomed. Opt*., **16** (4), 040503 (2011).
38. Welzel J., Bruhns M., Wolff H.H. *Arch. Dermatol. Res*., **295**, 50 (2003).
39. Stamatas G.N., Southall M., Kollias N. *J. Invest. Dermatol*., **126**, 1753 (2006).
40. Wang X.-J., Milner T.E., Chang M.C., Nelson J.S. *J. Biomed. Opt*., **1** (2), 212 (1996).
41. Meek K.M., Dennis S., Khan S. *Biophys. J*., **85** (4), 2205 (2003).